S1 Statistical surface temperature reconstructions from Stenni et al. (2017)

Based on the δ^{18}O composites, Stenni et al. (2017) reconstructed regional surface temperature over the last two millennia based on the statistical relationship between δ^{18}O and surface temperature. Three methods have been used to scale the δ^{18}O composites. In the first approach, the regional slopes between δ^{18}O and temperatures were computed from the outputs of the ECHAM5-wiso model forced by ERA-Interim atmospheric reanalysis (Goursaud et al., 2018) over the 1979–2013 period. In the second method, the reconstruction obtained from the first method for the WAIS region is corrected using an independent temperature record: the borehole temperature reconstruction at WAIS divide (Orsi et al., 2012). This allows to match the cooling trend over the 1000–1600 period (Stenni et al., 2017). This method provides a different reconstruction for the WAIS region – implying thus also the West Antarctic and the whole Antarctic reconstructions –, but not for the regions in East Antarctica. Finally, in the third method, the regional normalized δ^{18}O composites have been scaled to the variance of the surface temperature observations (e.g. Nicolas and Bromwich, 2014) over the 1960–1990 period. The second reconstruction is used throughout this study for two reasons: 1) the third method is based on the surface temperature observations, which are used here to estimate the skill of the reconstructions which could lead to a bias; 2) the correction introduced in the second method is expected to improve the reconstruction compared to the previous method. The temporal resolution of these surface temperature reconstruction is the same as the δ^{18}O composites: 10 years for 0–1800 period and 5 years for 1800–2010 period.

S2 Defining uncertainties associated with proxy data used during data assimilation process

Data assimilation requires estimates of the uncertainty associated with the proxy data used. Unfortunately, uncertainty estimations are not provided with the used published reconstructions and the instrumental time series are too short to reliably derive the uncertainty. If we apply the same error for all the Antarctic regions, the assimilation will tend to give more weight to the time series that have more variance (i.e. the high-accumulation regions). On the other hand, if we apply an error proportional to the standard deviation of the time series, each region will tend to have the same weight. The uncertainly could also be related to the number of ice cores included in each regional composite, but the link between this number and the quality of the composite is not straightforward (Stenni et al., 2017). Several experiments have been performed to test the impact of different estimates of the data uncertainties on the data assimilation results. The results are qualitatively similar for standard choices of the uncertainty (Klein et al., 2019). The experiments shown here assume a signal to noise ratio of 1 for each regional composite. This is probably an optimistic estimate but this has the advantage of providing a strong data constraint and the comparison of the reconstruction using data assimilation with instrumental data indicates a good skill of the methods using this value.

S3 Additional figures

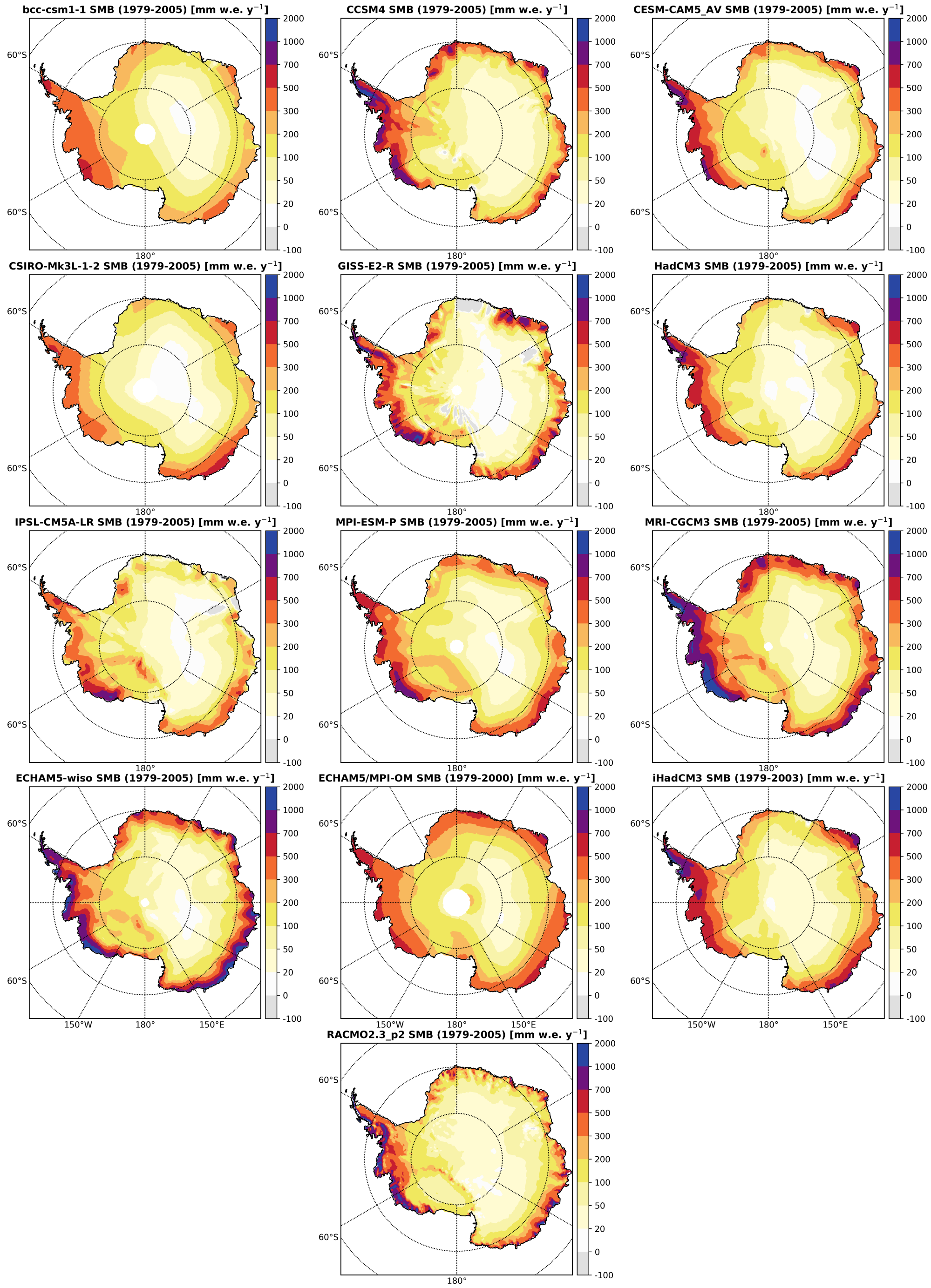

Figure S1 Antarctic Ice Sheet surface mass balance [mm w.e. y^{-1}] for all the models used in this study over the 1979–2005 period.

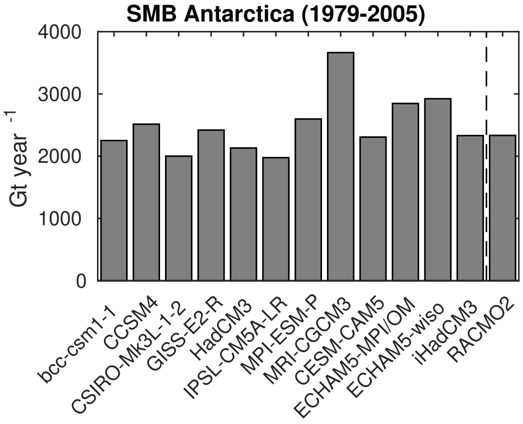

Figure S2 Mean Antarctic Ice Sheet surface mass balance (Gt year^{-1}) simulated by all the models used in this study.

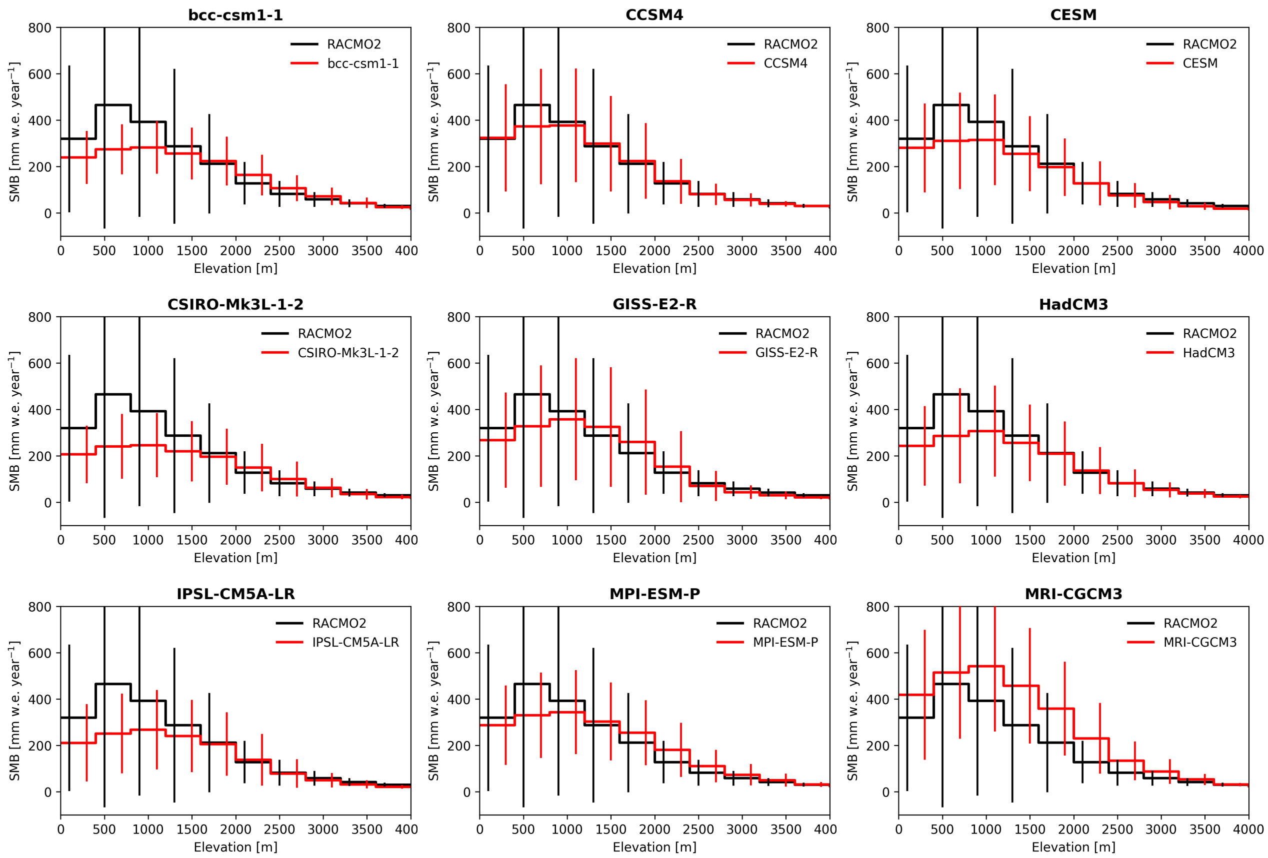

Figure S3 Distribution of the surface mass balance simulated by each GCM used in this study as a function of elevation, binned in 400m elevation intervals. The bars represent one standard deviation of the cell grids within each elevation bin.

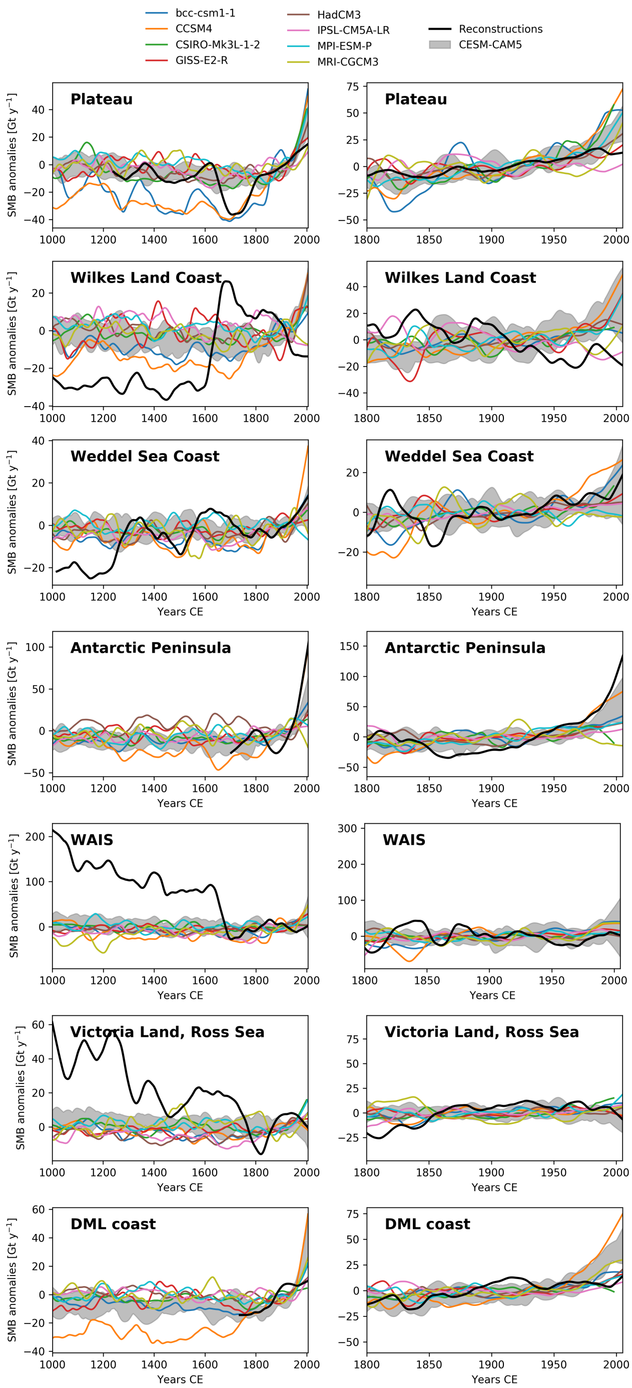

Figure S4 Surface mass balance anomalies [Gt y^{-1}] simulated by the GCMs (the average of all the available simulations has been represented; Tab. A1) and snow accumulation reconstructions (Thomas et al., 2017) for 1000–2005 and for 1800–2005 for all the Antarctic subregions. Anomalies are computed for the period 1800–2000. The shaded area corresponds to the range of the CESM1-CAM5 simulations. For visibility, data has been smoothed with a 100 year moving average for the last millennium and a 30 years moving average for the last 200 years.

Table S1 Surface mass balance trends (in Gt 100y^{-2}) for West Antarctica, East Antarctica and Antarctica as a whole in GCMs, in isotopic climate models (ECHAM5-wiso, ECHAM5/MPIOM and HadCM3) and in reconstructions based on ice cores (Thomas et al., 2017) over 1950–2000. The number in brackets is the number of simulations. The trend computation is based on yearly data.

	West Antarctica			East Antarctica			Antarctica		
	min	max	mean	min	max	mean	min	max	mean
bcc-csm1-1 (3)	-29.46	152.47	77.62	-63.11	381.09	200.39	-92.57	533.56	278.01
CCSM4 (6)	148.02	390.50	234.13	274.32	455.65	368.19	469.24	846.15	602.32
CSIRO-Mk3L-1-2 (1)			3.14			135.86			139.00
GISS-E2-R (6)	25.69	183.66	107.27	-71.92	250.18	140.43	-46.23	416.21	247.71
HadCM3 (10)	4.79	150.27	70.75	-68.85	242.18	89.39	-34.18	303.11	160.14
IPSL-CM5A-LR (6)	57.07	123.78	99.07	-104.18	66.82	-10.06	-47.11	174.30	89.01
MPI-ESM-P (2)	-33.85	-28.74	-31.30	54.75	231.84	143.29	26.01	197.99	112.00
MRI-CGCM3 (3)	28.62	178.64	86.45	-59.28	242.24	125.66	-7.19	420.89	212.11
CESM1-CAM5 (12)	30.90	349.67	153.07	55.72	340.24	162.27	161.99	592.43	315.34
iHadCM3 (6)	76.23	232.69	162.29	15.52	350.87	213.61	115.85	542.61	375.90
ECHAM5-wiso (1)			-8.79			195.22			186.43
ECHAM5/MPIOM (1)			41.44			35.43			76.87
Reconstructions (1)			256.74			-35.80			220.95

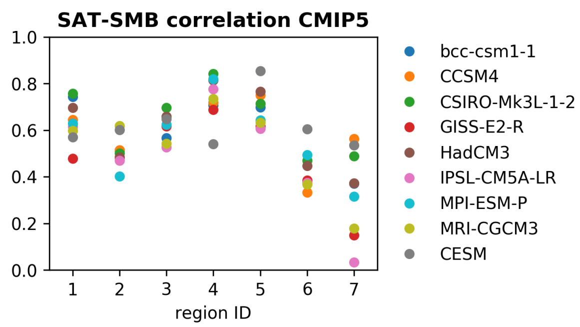

Figure S5 Annual correlations (r) between surface mass balance and surface temperature for all seven Antarctic regions (see Fig. 1 for geographical definitions) for all the GCMs over the 1850–2005 AD. "1" is for the Plateau and "7" for DML Coast.

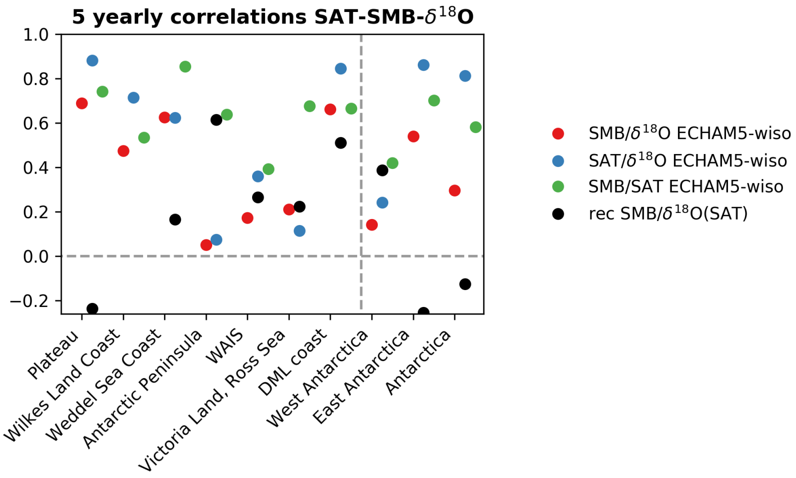

Figure S6 5 year correlations between SMB and δ^{18}O, surface temperature and δ^{18}O and, SMB and surface temperature for the seven Antarctic regions over 1870–199 time period from the ECHAM5-wiso outputs. In black, the correlation between the SMB reconstructions from Thomas et al. (2017) and the δ^{18}O of the Antarctic ice cores aggregated for the seven Antarctic regions (Stenni et al., 2017).

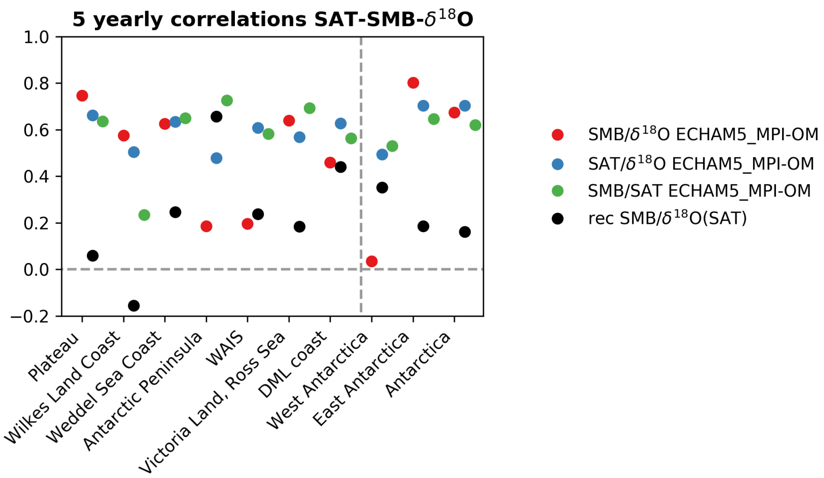

Figure S7 5 year correlations between SMB and δ^{18}O, surface temperature and δ^{18}O and, SMB and surface temperature for the seven Antarctic regions over 1850–1995 from the ECHAM5/MPI-OM outputs. In black, the correlation between the SMB reconstructions from Thomas et al. (2017) and the δ^{18}O of Antarctic ice cores aggregated for the seven Antarctic regions (Stenni et al., 2017).

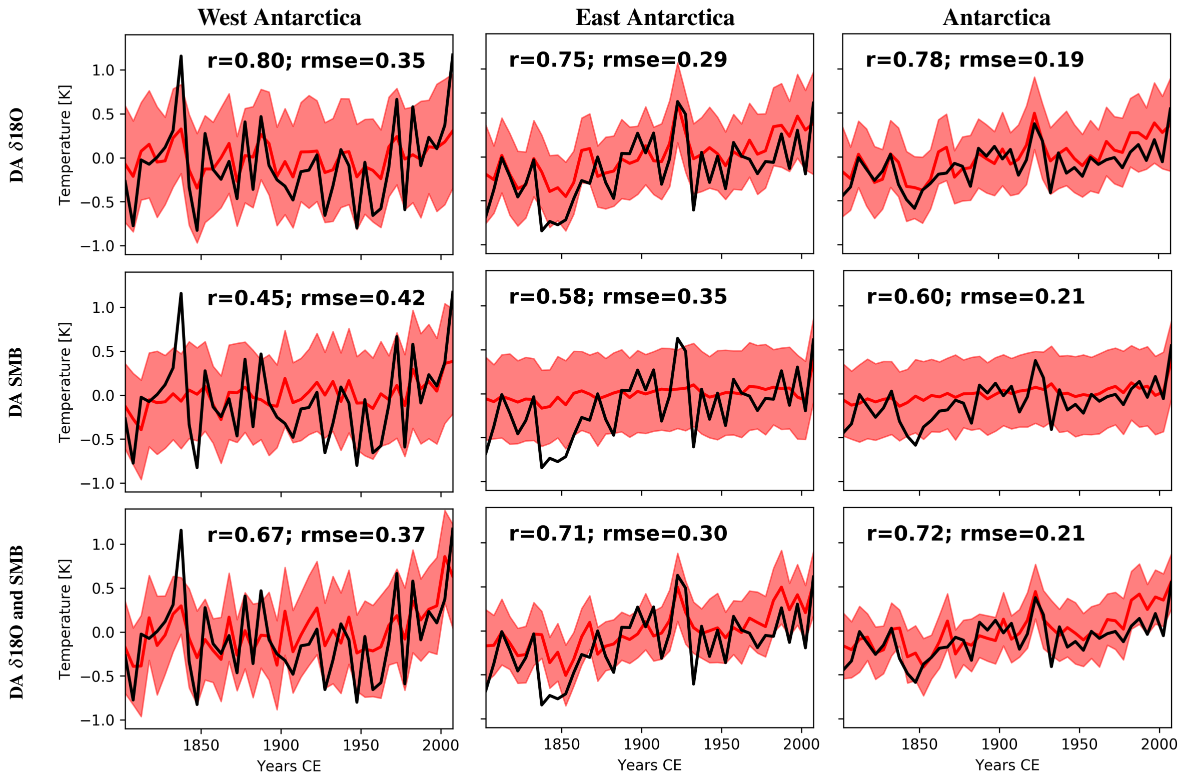

Figure S8 Reconstructed surface temperatures (5-year mean) for West Antarctica, East Antarctica and Antarctica as a whole from our data assimilation experiment using the ECHAM5-wiso outputs and, δ018 (Stenni et al., 2017) and SMB reconstruction (Thomas et al., 2017) as data. The period is 1800–2010. *DA* $\delta^{18}O$ is the data assimilation experiment using only the δ^{18}O data to constrain the model while *DA SMB* uses only the SMB reconstruction and *DA* $\delta^{18}O$ *and SMB* uses both. For each experiment and each region, the correlation (r) between the reconstruction based on ice cores and that based on data assimilation is computed. The shaded areas represent $\pm$ 1 standard deviation of the model particles.

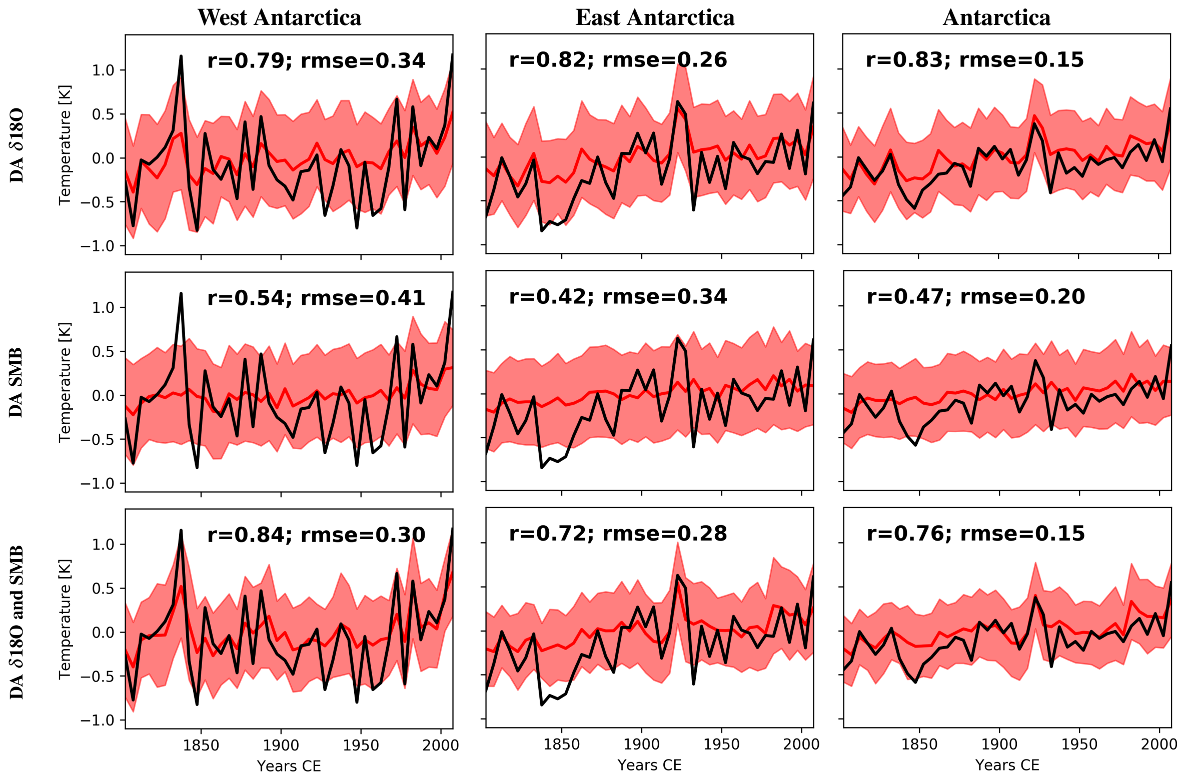

Figure S9 Reconstructed surface temperatures (5-year mean) for West Antarctica, East Antarctica and Antarctica as a whole from data assimilation experiment using the ECHAM5-MPI/OM outputs and, δ018 (Stenni et al., 2017) and SMB reconstruction (Thomas et al., 2017) as data. The period is 1800–2010. *DA* $\delta^{18}O$ is the data assimilation experiment using only the δ^{18}O data to constrain the model while *DA SMB* uses only the SMB reconstruction and *DA* $\delta^{18}O$ *and SMB* uses both. For each experiment and each region, the correlation (*r*) between the reconstruction based on ice cores and that based on data assimilation is computed. The shaded areas represent ± 1 standard deviation of the model particles.

Table S2 Slopes (°C $100yr^{-1}$) of each surface temperature reconstruction (Stenni et al., 2017; Klein et al., 2019; Nicolas and Bromwich, 2014; in this study) over the 1961–2010 period for West Antarctica, East Antarctica and the Antarctica. Statistically significant (p-value < 0.05) trends are represented by a star.

Dataset	West Antarctica	East Antarctica	Antarctica
Stenni et al. (2017)			
Stat ECHAMvariance	1.69*	0.75*	1.27
Stat borehole	2.07*	0.75*	0.77*
Klein et al. (2018)			
DA ECHAM5-wiso	1.15	0.94	0.98
DA ECHAM5/MPI-OM	1.0	0.48	0.59
Nicolas and Bromwich (2014)			
	2.22*	0.53	0.90*
In this study			
DA δ^{18}O and SMB iHadCM3	0.99*	0.60*	0.69*

Table S3 5-year mean correlations between the three surface temperature reconstructions from data assimilation experiments using the ECHAM5-MPI/OM outputs, ECHAM5-wiso outputs and the iHadCM3 outputs, and the surface temperature reconstructions from Nicolas and Bromwich (2014) over the 1958–2010 for the East, West and the whole Antarctica.

	West Antarctica			East Antarctica			Antarctica		
	ECHAM5-MPI/OM	ECHAM5-wiso	iHadCM3	ECHAM5-MPI/OM	ECHAM5-wiso	iHadCM3	ECHAM5-MPI/OM	ECHAM5-wiso	iHadCM3
DA δ^{18}O	0.57	0.78	0.69	0.19	0.08	0.13	0.50	0.47	0.34
DA SMB	0.40	0.52	0.55	0.27	0.53	0.60	0.28	0.58	0.65
DA δ^{18}O and SMB	0.53	0.65	0.72	0.34	0.48	0.61	0.59	0.71	0.73
Stenni et al. (2017)		0.79			0.10			0.57	

Table S4 5-year mean correlations between the three surface temperature reconstructions from data assimilation experiments using the iHadCM3 outputs and the statistical reconstruction of Stenni et al. (2017), with the surface temperature reconstructions from Nicolas and Bromwich (2014) over the 1958–2010 period for East Antarctica, West Antartica and Antarctica as a whole. All the correlations are performed on detrended time series. Stars represent statistically significant correlations (p-value<0.10).

	West Antarctica	East Antarctica	Antarctica
DA δ^{18}O	-0.02	-0.16	-0.25
DA SMB	-0.19	0.51	0.31
DA δ^{18}O and SMB	0	0.60*	0.44
Stenni et al. (2017)	0.45*	-0.20	0.12*

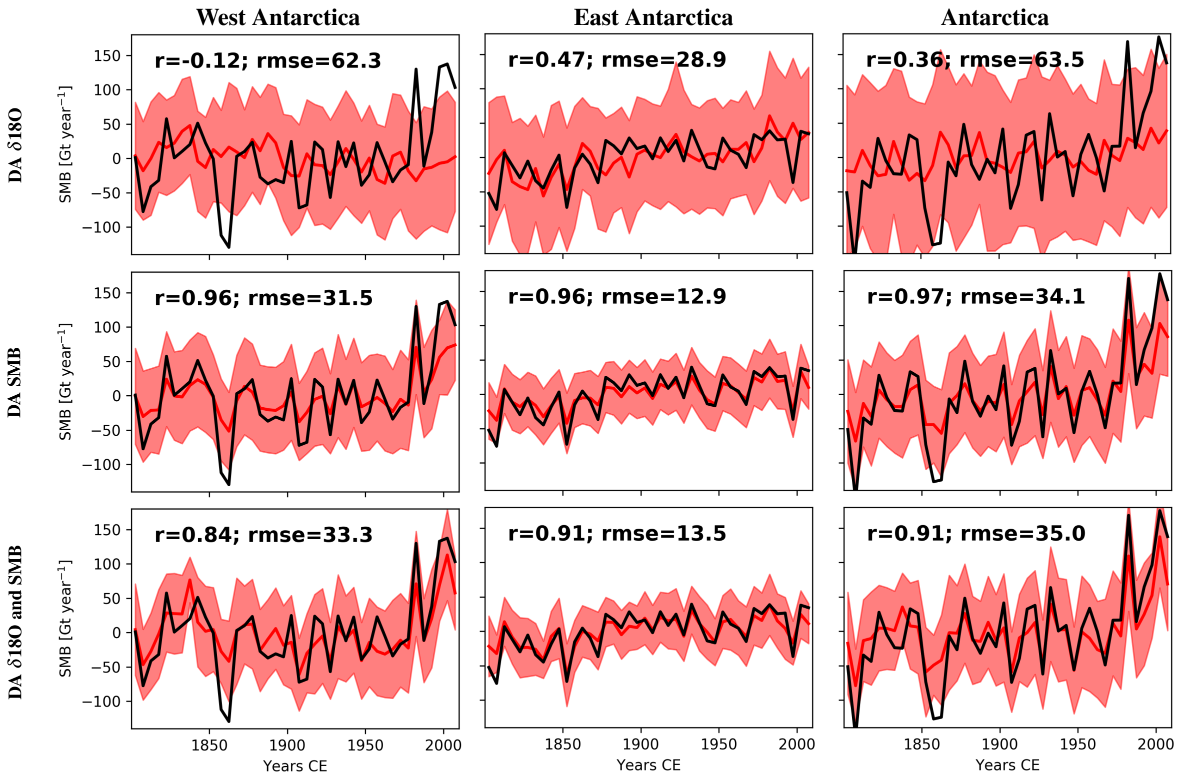

Figure S10 Reconstructed SMB (5-year mean) for West Antarctica, East Antarctica and Antarctica as a whole from data assimilation experiment using the ECHAM5-wiso outputs and, δ018 (Stenni et al., 2017) and SMB reconstruction (Thomas et al., 2017) as data. The period is 1800–2010. *DA* $\delta^{18}O$ is the data assimilation experiment using only the δ^{18}O data to constrain the model while *DA SMB* uses only the SMB reconstruction and *DA* $\delta^{18}O$ *and SMB* uses both. For each experiment and each region, the correlation (r) between the reconstruction based on ice cores and that based on data assimilation is computed. The shaded areas represent $\pm$ 1 standard deviation of the model particles.

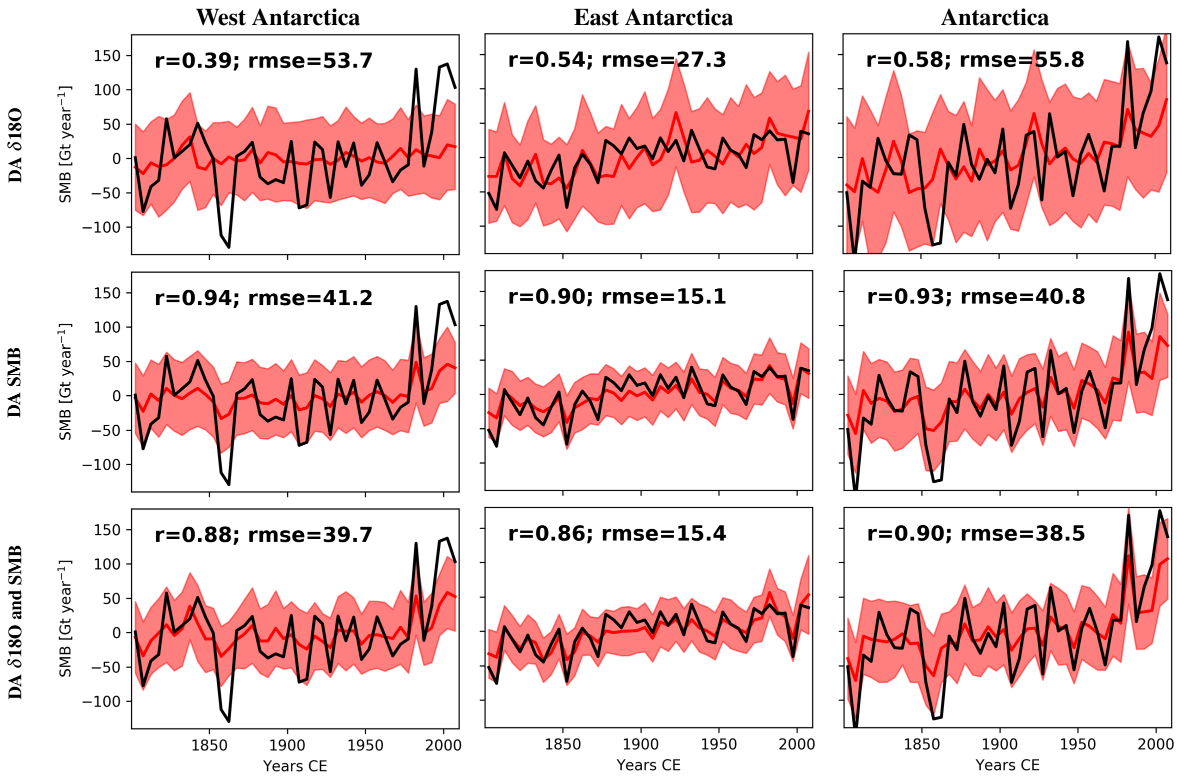

Figure S11 Reconstructed SMB (5-year mean) for West Antarctica, East Antarctica and Antarctica as a whole from data assimilation experiment using the ECHAM5-MPI/OM outputs and, δ018 (Stenni et al., 2017) and SMB reconstruction (Thomas et al., 2017) as data. The period is 1800–2010. *DA* $\delta^{18}O$ is the data assimilation experiment using only the δ^{18}O data to constrain the model while *DA SMB* uses only the SMB reconstruction and *DA* $\delta^{18}O$ *and SMB* uses both. For each experiment and each region, the correlation (r) between the reconstruction based on ice cores and that based on data assimilation is computed. The shaded areas represent $\pm$ 1 standard deviation of the model particles.

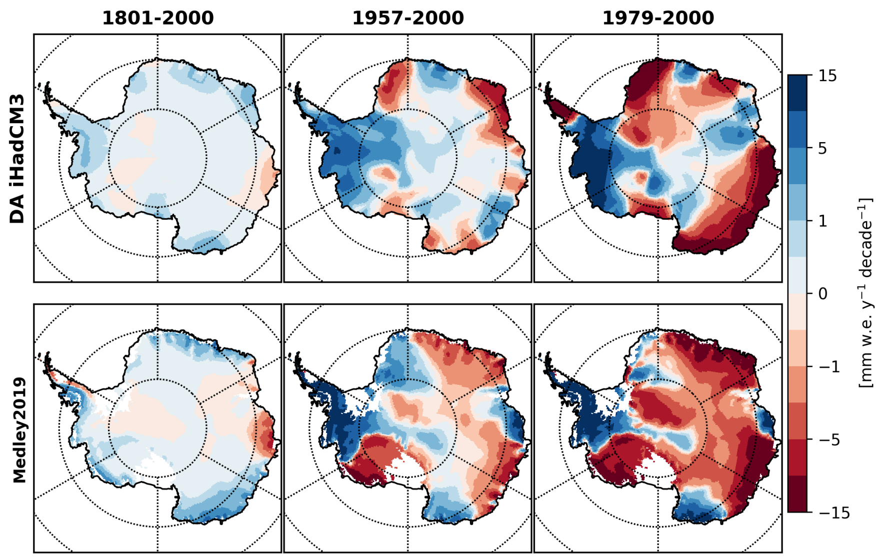

Figure S12 Spatial Antarctic surfance mass balance trends (mm w.e. y^{-1} decade^{-1}) over the 1801–2000, 1957–2000 and 1979–2000 periods from 1) our data assimilation-based reconstruction using the iHadCM3 outputs constrained by both δ^{18}O and SMB (first row) and from 2) Medley and Thomas (2019; second row).

References

Goursaud, S., Masson-Delmotte, V., Favier, V., Orsi, A., and Werner, M. (2018). Water stable isotopes spatio-temporal variability in Antarctica in 1960–2013: observations and simulations from the ECHAM5-wiso atmospheric general circulation model. *Climate of the Past Discussions*, 14:923–946.

Klein, F., Abram, N. J., Curran, M. A. J., Goosse, H., Goursaud, S., Masson-Delmotte, V., Moy, A., Neukom, R., Orsi, A., Sjolte, J., Steiger, N., Stenni, B., and Werner, M. (2019). Assessing the robustness of Antarctic temperature reconstructions over the past two millennia using pseudoproxy and data assimilation experiments. *Climate of the Past*, 15:661–684.

Medley, B. and Thomas, E. R. (2019). Increased snowfall over the antarctic ice sheet mitigated twentieth-century sea-level rise. *Nature Climate Change*, 9(1):34–39.

Nicolas, J. P. and Bromwich, D. H. (2014). New reconstruction of antarctic near-surface temperatures: Multidecadal trends and reliability of global reanalyses. *Journal of Climate*, 27(21):8070–8093.

Orsi, A. J., Cornuelle, B. D., and Severinghaus, J. P. (2012). Little Ice Age cold interval in West Antarctica: Evidence from borehole temperature at the West Antarctic Ice Sheet (WAIS) Divide. *Geophysical Research Letters*, 39(9):1–7.

Stenni, B., Curran, M. A., Abram, N. J., Orsi, A., Goursaud, S., Masson-Delmotte, V., Neukom, R., Goosse, H., Divine, D., Van Ommen, T., Steig, E. J., Dixon, D. A., Thomas, E. R., Bertler, N. A., Isaksson, E., Ekaykin, A., Werner, M., and Frezzotti, M. (2017). Antarctic climate variability on regional and continental scales over the last 2000 years. *Climate of the Past*, 13(11):1609–1634.

Thomas, E. R., Melchior Van Wessem, J., Roberts, J., Isaksson, E., Schlosser, E., Fudge, T. J., Vallelonga, P., Medley, B., Lenaerts, J., Bertler, N., Van Den Broeke, M. R., Dixon, D. A., Frezzotti, M., Stenni, B., Curran, M., and Ekaykin, A. A. (2017). Regional Antarctic snow accumulation over the past 1000 years. *Climate of the Past*, 13(11):1491–1513.